Modular Isolated Vertically Symmetric Dual Inductor Hybrid Converter For Differential Power Processing

Ratul Das and Hanh-Phuc Le
Department of Electrical and Computer Engineering, University of California San Diego
La Jolla, California, USA
{ratuldas, hanhphuc}@ucsd.edu

2021 IEEE Energy Conversion Congress and Exposition (ECCE) | 978-1-7281-5135-9/21/$31.00 ©2021 IEEE | DOI: 10.1109/ECCE47101.2021.9595908

***Abstract*—In this paper, a new isolated DC-DC converter is proposed and demonstrated for Point-Of-Load (POL) applications in data centers. The converter includes a novel architecture where a stacked switched-capacitor (SC) stage provides an efficient course step-down and reduces the voltage swing for the transformer and inductive stage. Compared with a conventional Dickson SC converter, the new SC stage features an advantageous 2X reduction in maximum operating voltage for flying capacitors, enabling capacitor size reduction. Through the transformer, two inductors at the output stage provide soft-charge and soft-discharge operations for the primary side flying capacitors and ensure a lossless capacitive power transfer operation. To support higher input voltages and larger conversion ratios, multiple modules of the proposed converter can be stacked in a series-input/parallel-output configuration. This modular architecture provides advantages of differential power processing with reduced input voltage and processed power for each converter module. A prototype of the modular architecture has been demonstrated for a 100V-to-3V point-of-load conversion with a maximum load of 60A. The peak efficiency of 91% is achieved at 57W/20A output.**

***Index Terms*—Hybrid Converter, Switched Capacitor, Multi Inductor Converter, Isolated, Modular, Capacitor Sizing.**

I. Introduction

DC-DC converters with large conversion ratios are required in many applications, such as automotive, data centers, solar plants, etc. Recently, the demand for high voltage buses has been much more severe because of the increased current from or to the bus for high demand on the user's end, leading to significant relevant efforts from the industry and academia.

In data centers, last-centimeter conversion capable of supplying a moderate conversion ratio of 48V to 1-3.3V is desirable in recent emerging power delivery architecture. Recent demonstrations of different non-isolated DC-DC converter topologies for this application include a two-stage architecture with a 12V intermediate bus in [1] or a single-stage direct-conversion solution from 48V to core voltages in [2], [3]. In the non-isolated category, these solutions are switched-capacitor-based hybrid converters with or without regulation [1], [2]. In the isolated category, LLC and ICN-based converter have been also demonstrated [3]–[6]. In this work, we are proposing a new architecture with a combination of switched-capacitor and transformer stages. The switched capacitor (SC) stage tolerates the high input voltage while the transformer stage provides isolation capability. In this design, to improve the output current capability a current doubler rectifier is employed at the secondary side of the transformer. The converter architecture is called Isolated Vertically Symmetric Dual Inductor Hybrid (IVS-DIH) converter as it has two output inductors and symmetric configuration across its vertical center. The switched capacitor portion tolerates symmetrical voltages at the two terminals of the transformer's primary.

Section II discusses the converter topology, operation, and steady-state analysis. Multiple modules of the converter can also be stacked to get the benefits of differential power processing. This stacked input/parallel output modular architecture is presented in section III. Section IV lists the experimental results obtained. The paper is summarized and concluded in section V.

II. Topology

A. Derivation

Multi-level Dual Inductor Hybrid (DIH) converters were first demonstrated for 48V-to-1V POL applications [7]–[9]. These converters provide seamless control of the output voltage with normal Buck-like pulse width modulated (PWM) duty cycle control. Fig. 1a shows a 4-level DIHC converter with a conversion ratio of $^{DV_{in}}/_{4}$. These converters can be utilized in applications that require large conversion ratios. However, the drawback of this converter family is that it requires a large bias voltage for the top capacitors, leading to capacitance degradation due to high DC voltage bias and larger capacitor sizes, which in turn, lead to limits in efficiency and/or power density [9].

To reduce the voltage stress and completely remove hard-charging on flying capacitors. Fig. 1b shows the configuration where, output, inductors, and free-wheeling switches are placed midway between the positive and negative rails of the input. These components are functionally isolated from the main switched capacitor architecture with the flying capacitors. If these capacitors can be chosen as safety rated, this converter can be used as an isolated converter. However, safety-rated capacitors typically have small values while high current applications require much larger capacitance for proper voltage operations in multi-level hybrid converters. Fig. 1b shows a dual inductor hybrid converter where the output

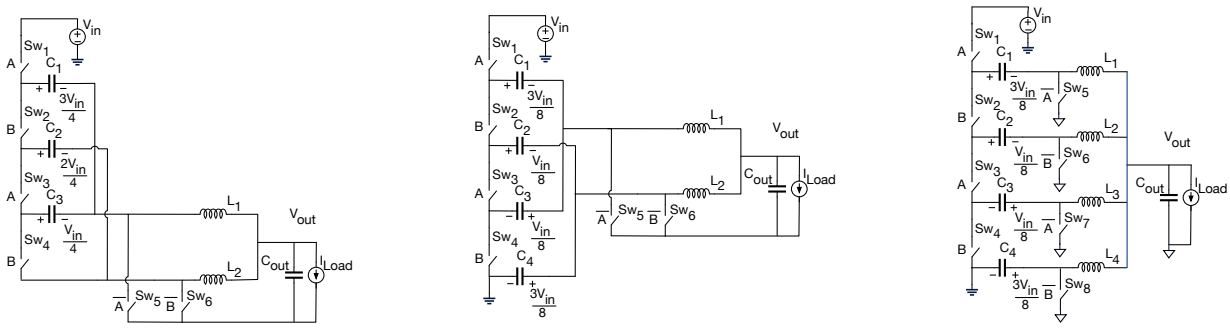

(a) 4-level Dual Inductor Hybrid (DIH) converter

(b) 4-level Vertically Symmetric Dual Inductor Hybrid (VS-DIH) converter

(c) 4-level Vertically Symmetric Multi Inductor Hybrid (VS-MIH) converter

Figure 1: Derivation of the Vertically Symmetric Dual Inductor Hybrid (IVS-DIH) and Multi Inductor Hybrid (IVS-MIH) converter

and voltage distribution on the flying capacitors is vertically symmetric. Following the same derivation of Multi Inductor Hybrid (MIH) topologies in [8]–[12], multiple inductors can also be arranged at the output to support large output currents. The configuration is shown in Fig. 1c.

In order to provide a proper safety-rated isolation and additional voltage conversion, a transformer can be inserted between the switched capacitor architecture and the output inductive stage, which results in the circuit shown in Fig. 2. The input switched capacitor stage of this converter consists of four switches, Sw_{1-4} and four capacitors, C_{1-4}. In the secondary side, there are two switches Sw_{5-6} and two inductors L_{1-2} forming a current doubler rectifier. Following this converter architecture, the transformer and secondary inductive stage can be other well-known isolated converters such as LLC, Impedance Control Network (ICN), etc. [3].

B. Operation

The converter is operated with two 180°phase-shifted signals, A and B, in the primary side and their inverted signals, $\overline{\text{A}}$ and $\overline{\text{B}}$, in the secondary side. It is possible to control, regulate and change the output voltage by changing the duty cycles of A and B phases up to the maximum value of ∼50%. In this demonstration, we target to operate the converter at near 50% duty cycle, yielding two operating states shown in Figs. 3a and 3b. In these operating states, red color indicates components being charged and blue color for components being discharged. The operation of the converter can be explained using these two figures along with the timing diagram shown in Fig. 4.

During state 1, the on-time of phase A, switches $Sw_{1,3}$ in the SC architecture and Sw_6 in the secondary side are ON, while other switches $Sw_{2,4,5}$ are kept OFF. In the SC architecture, current starts flowing through the capacitors by charging capacitors C_1 and C_4 and discharging capacitors $C_{2,3}$. The charging current of C_1 and discharging current of C_3 combines and flows through the primary side of the transformer and split into two parts to discharge C_2 and charge C_4. The voltage and current of the primary side of the transformer are induced to the secondary side to charge the inductor L_1. Sw_5 provides a path for the secondary current of the transformer as well the free-wheeling current of L_2. As the charging and discharging currents of the capacitors are reflected to the secondary side and eventually flow through L_1, this operation makes sure the capacitors are being softly charged and discharged.

State 2 is complementary of state 1. $Sw_{2,4,5}$ are ON and

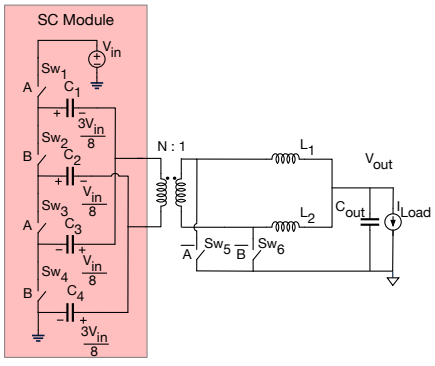

Figure 2: 4-level Isolated Vertically Symmetric Dual Inductor Hybrid (IVS-DIH) converter

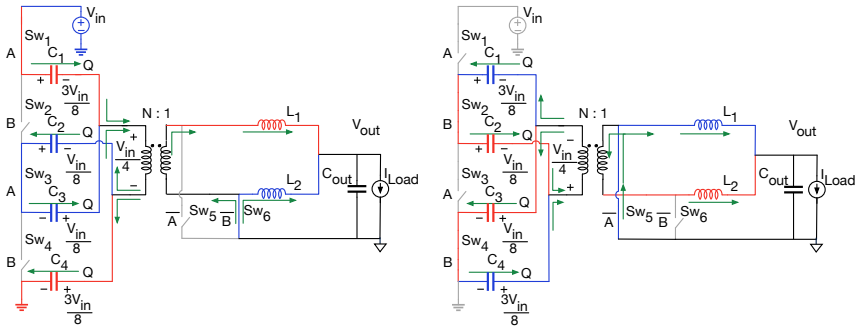

(a) State 1

(b) State 2

Figure 3: Operation of the converter (Red color for charging and Blue color for discharging components)

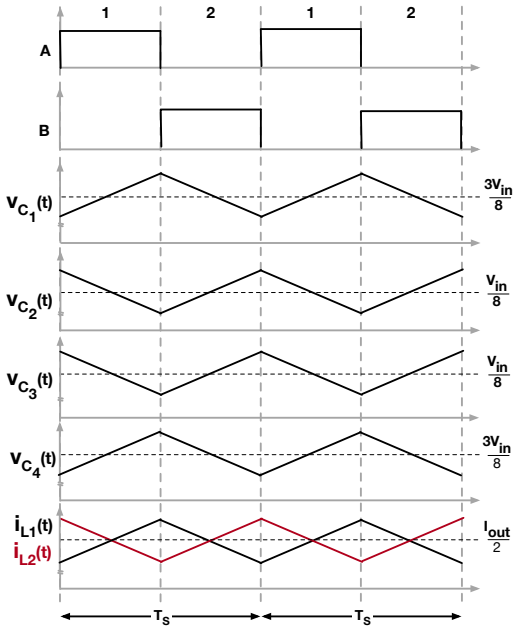

Figure 4: Ideal timing diagram of the operation

the other switches are OFF. This configuration allows the charged capacitors of state 1, $C_{1,4}$, to discharge and discharged capacitors of state 1, $C_{2,4}$, to charge. The combined current flow in the reverse direction of the transformer's primary side compared to state 1. The reflected current in the secondary flows through the inductor L_2. L_2 ensures the soft-charging of $C_{2,3}$ and soft-discharging of $C_{1,4}$. During this state, Sw_5 carries the transformer current and the free-wheeling current of L_1.

C. Steady-State Analysis

Considering the duty-cycle D of phases A and B and transformer turn ratio N:1, we can get the following equations by applying volt-second balance on the inductors L_{1-2}:

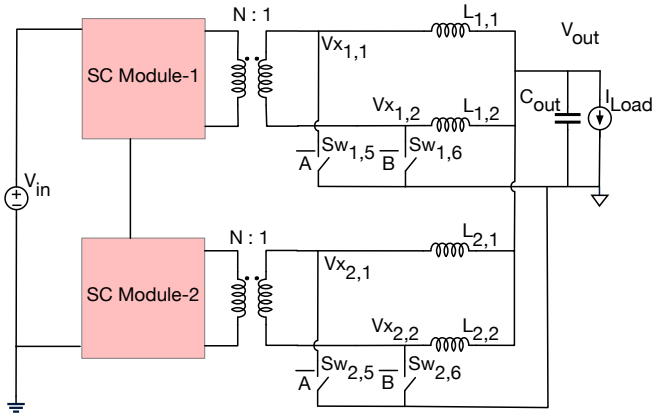

Figure 5: Modular architecture for differential power processing

$$\left[[V_{in}-(V_{C_1}+V_{C_4})]\frac{1}{N}-V_{out}\right]D-V_{out}(1-D)= \left[[(V_{C_2}+V_{C_3})]\frac{1}{N}-V_{out}\right]D-V_{out}(1-D)=0 \quad (1)$$

$$\left[[(V_{C_1}-V_{C_2})]\frac{1}{N}-V_{out}\right]D-V_{out}(1-D)= \left[[(V_{C_4}-V_{C_3})]\frac{1}{N}-V_{out}\right]D-V_{out}(1-D)=0 \quad (2)$$

Using equation 1 and 2, the conversion ratio and the capacitor voltages can be derived as,

$$V_{out}=\frac{DV_{in}}{4N},\ V_{C_1}+V_{C_4}=\frac{3V_{in}}{4} \text{ and } V_{C_2}+V_{C_3}=\frac{V_{in}}{4} \quad (3)$$

The individual voltages on the capacitors can be calculated as,

$$V_{C_1}=\frac{C_4}{C_1+C_4}\frac{3V_{in}}{4},\ V_{C_2}=\frac{C_3}{C_2+C_3}\frac{V_{in}}{4},\ V_{C_3}=\frac{C_2}{C_2+C_3}\frac{V_{in}}{4} \text{ and } V_{C_4}=\frac{C_1}{C_1+C_4}\frac{3V_{in}}{4} \quad (4)$$

As an equitable voltage bias on the capacitors are wanted, capacitors can be chosen so that, $C_1=C_4$ and $C_2=C_3$. This choice will ensure a balanced operation in the switched capacitor architecture with,

$$V_{C_1}=\frac{3V_{in}}{8},\ V_{C_2}=\frac{V_{in}}{8},\ V_{C_3}=\frac{V_{in}}{8} \text{ and } V_{C_4}=\frac{3V_{in}}{8} \quad (5)$$

Based on the derived capacitor voltages and considering small ripples, the maximum voltage stress on the switches, Sw_{1-4} are $V_{in}/2$. Secondary-side switches, Sw_{5-6} experience a voltage stress of $V_{in}/4N$.

The division by 4 in the conversion ratio in Eqn. 3 comes from the number of switched-capacitor levels. In this particular demonstration, we have restricted the operation of the converter to D=50% with the transformer's turn ratio of 4:2, the conversion ratio becomes in total, 16. If a higher conversion ratio is required, either the transformer turn ratio or the levels in the SC architecture can be increased.

For a converter with L number of SC levels with L stack switches and L capacitors, and N:1 transformer, the conversion ratio and the capacitor voltages can be calculated as:

$$V_{out}=\frac{DV_{in}}{LN} \text{ and } V_{C_k}=V_{C_{L-k+1}}=\frac{[L-(2k-1)]V_{in}}{2L}, \text{ where, k } =1,2,3,...,\frac{L}{2} \quad (6)$$

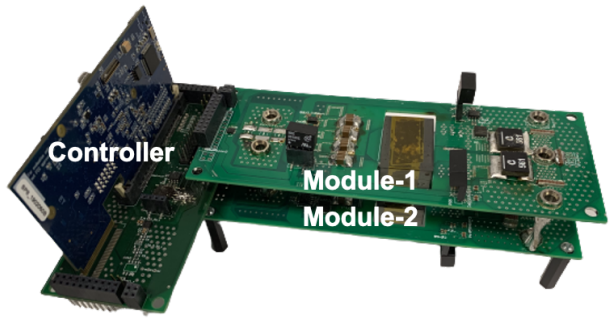

Figure 6: DC-stack modular configuration with two modules

Table I: List of Components

Components	Parts
S_{1-6}	40V MOSFET (Infineon)
C_{1-4}	2x1.4 µF COG (KEMET)
Transformer	4:2 turn ratio with planar N97 ER32 core (EPCOS TDK)
$L_{1,2}$	560 nH (Coilcraft)
Gate driver	UCC5350MC

D. Capacitor Sizing

While conventional Dickson SC converter requires equal capacitor sizing for low loss operation [13], in Dickson-based hybrid converter, a new capacitor sizing method was proposed to ensure full soft-charging and soft-discharging of all flying capacitors [9]. This method bases on circuit branch impedance in the hybrid converter operation and requires significantly different capacitance values, which can lead to complications in selecting flying capacitors. In the converter presented in this paper, the transformer sees two capacitor branches comprised of series connected C_1 and C_4 in parallel with series connected C_2 and C_3 during State 1 in Fig. 3a). During the state 2 in Fig. 3b, the converter sees again two branches of capacitors, series connected C_1 and C_2 in parallel with series connected C_3 and C_4. To ensure same capacitance in each branch connected in any state, all the capacitance can be selected with the same value. This simplifies capacitor selection back to the simple equal capacitors in Dickson SC converter and eliminates the requirement of different capacitors in [9] or the complex split-phase operation in [14].

III. Modular Architecture For Differential Power Processing

As modern electrical power delivery requires higher voltage buses to reduce the distribution copper loss, converters are being exposed to higher and higher voltages. Although the input SC stage can increase the capacitor stages to support a higher input voltage, this also means there are more capacitors exposed to higher operating voltages. To mitigate this problem, a modular structure as shown in Fig. 5 can be used. In this structure, two converters of Fig. 2 can be connected in a stacked input/parallel output configuration. Each converter effectively only receives an input voltage of $V_{in}/2$ and processes half of the total output power. While the conversion ratio becomes $V_{out} = \frac{DV_{in}}{8N}$, DC bias voltages of each module's capacitors are reduced to $3V_{in}/16$ and $V_{in}/16$. For M number of modules of L SC levels with N:1 transformers, Eqn. 6 can be rewritten as,

$$V_{out} = \frac{DV_{in}}{MLN} \text{ and}$$
$$V_{C_k} = V_{C_{L-k+1}} = \frac{[L-(2k-1)]\,V_{in}}{2ML}, \quad (7)$$
$$\text{where, k } = 1, 2, 3, ..., \frac{L}{2}.$$

IV. Experimental Results

A proof-of-concept prototype of the converter in Fig. 2 is built using the components in Table I. Two modules of the converter are stacked as in Fig. 6 to demonstrate the modular architecture. Figure 7 shows the operation of the converter at 100V to 2.85V/20A with an operating frequency of 300kHz.

Figures 7b and 7c show the capacitor voltages of the converter. As most of the flying capacitors are floating, measurement probes are required to be placed across the capacitors rather than referencing to ground. Interestingly, capacitor voltages drift very slowly if measured with any single-ended or even differential probe. The leakage in the voltage probes introduces some extra charge loss in the converter which is responsible for this drifting. To overcome this problem, two similar differential probes have been used to measure the similar type of capacitor voltages so that the leakage from both the probes nullifies the resulted drifting each other. During the measurements, the voltages of the first module's flying capacitors C_1 and C_4, and C_2 and C_3 have been measured together. The same procedure was applied to measure the voltages of the second module's C_1 and C_4, and C_2 and C_3. Figures 7b and 7c show the capacitor voltages are balanced in the steady-state operation.

The measured performance of the converter is provided in Fig. 8a with its efficiency. Figure 8b shows its measured output voltage versus output current to illustrate its output resistance and conduction loss. The converter reached a peak efficiency of 91% for a 100V-to-2.85V/20A conversion. The converter's maximum output current was measured at 60A while the converter obtains 2.41V output voltage and achieves 82.1% efficiency. The regulation capability of the converter is also shown in Fig. 9 with regulated outputs of 2V and 1V with 87% and 83.15% peak efficiencies at 30A and 25A respectively.

V. Conclusion

In summary, this paper presents a new isolated hybrid converter architecture in which a new input SC stage that can be combined with traditional isolated solutions, e.g., current doubler rectifier, to exploit full benefits of both large courses step-down by the SC stage and fine output regulation and isolation by the transformer and inductive stage. This SC circuit is more advantageous compared with the traditional Dickson-based solution because the maximum capacitor voltage stress can be significantly reduced. To further reduce

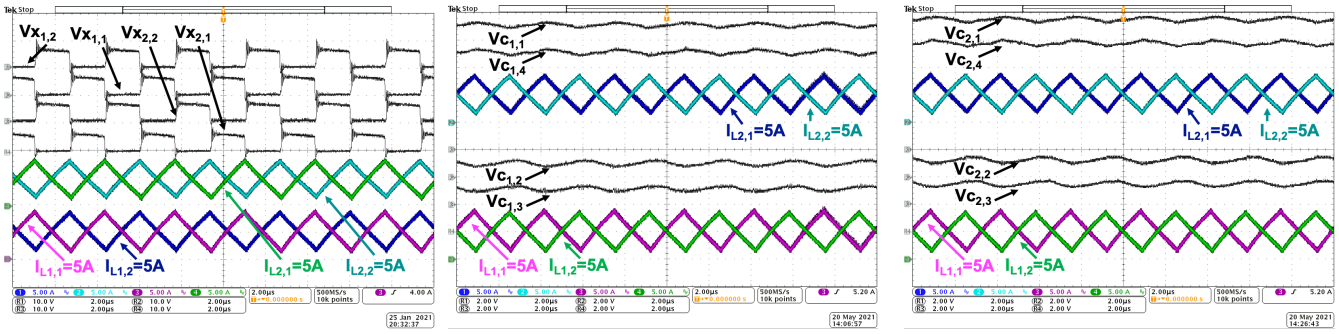

(a) Switching node voltage of the converter (b) Capacitor voltages of the first module (c) Capacitor voltages of the second module

Figure 7: Multi-module DC-stack operation at a 100V-to-2.85V/20A operation

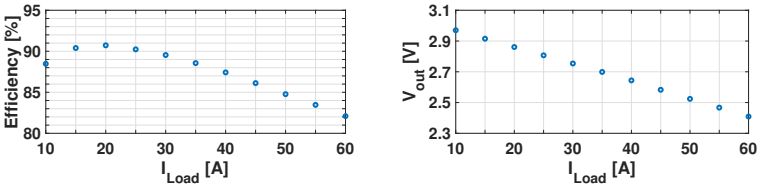

(a) Converter efficiency (b) Output voltage

Figure 8: Measured performance of the modular converter prototype with two DC-stack modules at 100V input voltage

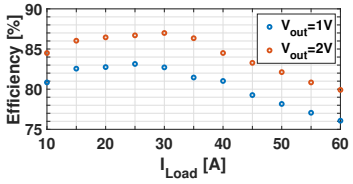

Figure 9: Measured efficiency of the converter at 100V input and regulated output voltages

the capacitor voltage stress, the modular architecture of the converter module can be utilized. The modular operation also provides the benefits of differential power processing to reduce the power stress for each converter module. A proof-of-concept converter prototype was implemented and measured for modular operation to support POL applications from 100V input. The modular operation reached a peak efficiency of 91% for 100V to 2.85V operation.

ACKNOWLEDGEMENT

We thank the National Science Foundation (NSF) of the United States for supporting the research in our group and funding this work under the NSF ECCS award No. 2043025 (previously No. 1810470). We also thank Casey Hardy and Tirthasarathi Lodh, who are PhD students at the ECE department of the University of California San Diego for their suggestions and help during the experiments.

REFERENCES

[1] J. Zhu and D. Maksimovic, "48 V-to-1 V Transformerless Stacked Active Bridge Converters with Merged Regulation Stage," in *2020 IEEE 21st Workshop on Control and Modeling for Power Electronics (COMPEL)*, Nov. 2020, pp. 1–6.

[2] J. S. Rentmeister and J. T. Stauth, "A 48V:2V flying capacitor multi-level converter using current-limit control for flying capacitor balance," in *2017 IEEE Applied Power Electronics Conference and Exposition (APEC)*, Mar. 2017, pp. 367–372.

[3] A. Kumar, S. Pervaiz, and K. K. Afridi, "High-Performance Single-Stage Isolated 48V-to-1.8V Point-of-Load Converter Utilizing Impedance Control Network and Distributed Transformer," in *2018 IEEE Energy Conversion Congress and Exposition (ECCE)*, Sep. 2018, pp. 3838–3843.

[4] M. H. Ahmed, M. A. de Rooij, and J. Wang, "High-Power Density, 900-W LLC Converters for Servers Using GaN FETs: Toward Greater Efficiency and Power Density in 48 V to 6\/12 V Converters," *IEEE Power Electronics Magazine*, vol. 6, no. 1, pp. 40–47, Mar. 2019.

[5] A. Kumar and K. K. Afridi, "Single-stage isolated 48V-to-1.8V point-of-load converter utilizing an impedance control network for wide input range operation," in *2017 IEEE Energy Conversion Congress and Exposition (ECCE)*, Oct. 2017, pp. 2003–2009.

[6] A. Kumar, S. Pervaiz, and K. K. Afridi, "Single-stage isolated 48V-to-1.8V point-of-load converter utilizing an impedance control network and integrated magnetic structures," in *2017 IEEE 18th Workshop on Control and Modeling for Power Electronics (COMPEL)*, Jul. 2017, pp. 1–7.

[7] S. Khatua, D. Kastha, and S. Kapat, "A Non-Isolated Single-Stage 48V-to-1V VRM with a Light Load Efficiency Improvement Technique," in *2018 IEEE Energy Conversion Congress and Exposition (ECCE)*, Sep. 2018, pp. 143–148.

[8] G.-S. Seo, R. Das, and H.-P. Le, "Dual Inductor Hybrid Converter for Point-of-Load Voltage Regulator Modules," *IEEE Transactions on Industry Applications*, vol. 56, no. 1, pp. 367–377, Jan. 2020.

[9] R. Das, G.-S. Seo, and H.-P. Le, "Analysis of Dual-Inductor Hybrid Converters for Extreme Conversion Ratios," *IEEE Journal of Emerging and Selected Topics in Power Electronics*, pp. 1–1, 2020.

[10] T. Xie, R. Das, G. Seo, D. Maksimovic, and H.-P. Le, "Multiphase Control for Robust and Complete Soft-charging Operation of Dual Inductor Hybrid Converter," in *2019 IEEE Applied Power Electronics Conference and Exposition (APEC)*, Mar. 2019, pp. 1–5.

[11] R. Das, G. Seo, D. Maksimovic, and H.-P. Le, "An 80-W 94.6%-Efficient Multi-Phase Multi-Inductor Hybrid Converter," in *2019 IEEE Applied Power Electronics Conference and Exposition (APEC)*, Mar. 2019, pp. 25–29.

[12] R. Das and H.-P. Le, "A Regulated 48V-to-1V/100A 90.9%-Efficient Hybrid Converter for POL Applications in Data Centers and Telecommunication Systems," in *2019 IEEE Applied Power Electronics Conference and Exposition (APEC)*, Mar. 2019, pp. 1997–2001.

[13] M. D. Seeman and S. R. Sanders, "Analysis and Optimization of Switched-Capacitor DC–DC Converters," *IEEE Transactions on Power Electronics*, vol. 23, no. 2, pp. 841–851, Mar. 2008.

[14] Y. Lei, R. May, and R. Pilawa-Podgurski, "Split-Phase Control: Achieving Complete Soft-Charging Operation of a Dickson Switched-Capacitor Converter," *IEEE Transactions on Power Electronics*, vol. 31, no. 1, pp. 770–782, Jan. 2016.